

Submitted to ApJL

Spitzer and ground-based infrared observations of the 2006 eruption of RS Ophiuchi

A. Evans¹, C. E. Woodward², L. A. Helton², R. D. Gehrz², D. K. Lynch³, R. J. Rudy³, R. W. Russell³, T. Kerr⁴, M. F. Bode⁵, M. J. Darnley⁵, S. P. S. Eyres⁶, T. R. Geballe⁷, T. J. O'Brien⁸, R. J. Davis⁸, S. Starrfield⁹, J.-U. Ness⁹, J. Drake¹⁰, J. P. Osborne¹¹, K. L. Page¹¹, G. Schwarz¹², J. Krautter¹³

ABSTRACT

We present Spitzer Space Telescope and complementary ground-based infrared observations of the recurrent nova RS Ophiuchi, obtained over the period

¹Astrophysics Group, Keele University, Keele, Staffordshire, ST5 5BG, UK, *ae@astro.keele.ac.uk*

²Department of Astronomy, School of Physics & Astronomy, 116 Church Street S.E., University of Minnesota, Minneapolis, MN 55455, USA, *chelsea@astro.umn.edu*, *ahelton@astro.umn.edu*, *gehrz@astro.umn.edu*

³The Aerospace Corporation, Mail Stop M2-266, P.O. Box 92957, Los Angeles, CA 90009-2957, USA, *David.K.Lynch@aero.org*, *Richard.J.Rudy@aero.org*, *Ray.Russell@aero.org*

⁴Joint Astronomy Centre, 660 N. A'ohoku Place, University Park, Hilo, Hawaii 96720, USA, *t.kerr@jach.hawaii.edu*

⁵Astrophysics Research Institute, Liverpool John Moores University, Twelve Quays House, Birkenhead CH41 1LD, UK, *mfb@astro.livjm.ac.uk*, *mjd@astro.livjm.ac.uk*

⁶Centre for Astrophysics, University of Central Lancashire, Preston, PR1 2HE, UK, *spseyres@uclan.ac.uk*

⁷Gemini Observatory, 670 N. A'ohoku Place, Hilo, HI 96720, USA, *tgeballe@gemini.edu*

⁸Department of Physics & Astronomy, University of Manchester, Manchester, UK, *tob@jb.man.ac.uk*, *rjd@jb.man.ac.uk*

⁹School of Earth & Space Exploration, Arizona State University, PO Box 871404, AZ 85287-1404, USA, *sumner.starrfield@asu.edu*, *ness@susie.la.asu.edu*

¹⁰Harvard-Smithsonian Center for Astrophysics (CfA), 60 Garden Street, Cambridge, MA 02138, USA, *jdrake@cfa.harvard.edu*

¹¹Department of Physics and Astronomy, University of Leicester, Leicester, LE1 7RH, UK, *julo@star.le.ac.uk*, *kpa@star.le.ac.uk*

¹²Steward Observatory, University of Arizona, 933 North Cherry Avenue, Tucson, AZ 85721, USA, *gschwarz@as.arizona.edu*

¹³Landessternwarte, Königstuhl, D-69117 Heidelberg, Germany, *j.krautter@lsw.uni-heidelberg.de*

64-111 days after the 2006 eruption. The Spitzer IRS data show a rich emission line spectrum superimposed on a free-free continuum. The presence of fine structure and coronal infrared lines lead us to deduce that there are at least two temperatures (1.5×10^5 K and 9×10^5 K) in the ejecta/wind environment, and that the electron density in the ‘cooler’ region is 2.2×10^5 cm $^{-3}$. The determination of elemental abundances is not straightforward but on the assumption that the Ne and O fine structure lines arise in the same volume of the ejecta, the O/Ne ratio is $\gtrsim 0.6$ by number.

Subject headings: stars: individual (RS Oph) — novae, cataclysmic variables — binaries: symbiotic — binaries: close — infrared: stars

1. Introduction

RS Oph is a recurrent nova (RN) that erupted in 1898, 1933, 1958, 1967, 1985, and possibly 1907 and 1945. The system consists of a semi-detached binary system comprised of a roche-lobe-filling giant (RG) and a massive ($\sim 1.2 M_\odot$) white dwarf (WD; Shore et al. 1996; Fekel et al. 2000). As in classical novae, the eruption follows a thermonuclear runaway on the surface of the WD (Starrfield et al. 1988). In the case of the RS Oph class of RNe, however, the ejected material runs into, and shocks, a dense RG wind (Bode & Kahn 1985).

The 1985 eruption of RS Oph was, for the first time, the subject of a multi-wavelength observational campaign, from the radio to the x-ray (Bode 1987). The most recent eruption, on 2006 February 12.83 (Hirosawa 2006, we take this to define the origin of time: $t = 0$), triggered an even more intensive campaign. Infrared (IR) observations by Das et al. (2006) and Evans et al. (2007, hereafter Paper I) show evidence for the shock, seen also at radio (O’Brien et al. 2006) and x-ray (Bode et al. 2006; Sokoloski et al. 2006; Ness et al. 2007; Osborne et al. 2007) wavelengths, as the ejecta interact with the RG wind. HST observations of the ejecta from the 2006 eruption (Bode et al. 2007) showed that emission in [O III]5007Å consists of two ‘rings’ consistent with constant velocity expansion of the radio lobes seen earlier in the eruption (O’Brien et al. 2006). In contrast the [Ne V]3426Å lines possibly arise from two ‘polar caps’ at the extremities of the rings.

We present here further IR observations, obtained with the Infrared Spectrometer (IRS; Houck et al. 2004) on the Spitzer Space Telescope (Werner et al. 2003; Gehrz et al. 2007) and from ground-based facilities.

2. Observations

2.1. Spitzer

RS Oph was observed on 2006 Apr 16 ($t = 62.51$ days) and 2006 Apr 26 ($t = 72.54$ days) with *Spitzer* IRS as part of the Directors Discretionary Time program PID 270. Observations were performed using all IRS modules, with IRS blue (13.3–18.6 μm) peak-up on RS Oph. The spectroscopy consisted of 5 cycles of 14 second ramps in short-low mode, 5 cycles of 30 second ramps in both short-high and long-low modes, and 5 cycles of 60 second ramps in long-high mode. IRS basic calibrated data products (BCDs) were processed with version 14.0.0 of the IRS pipeline. Details of the calibration and raw data processing are specified in the IRS Pipeline Description Document¹, version 1.0.

Bad pixels were interpolated in individual BCDs using bad pixel masks provided by the Spitzer Science Center (SSC). For the low resolution data, multiple data collection events were obtained at two different positions on the slit using *Spitzer*'s nod function. The low resolution two-dimensional BCDs were differenced to remove the background flux contribution and the data were extracted with SPICE (version 1.3-beta1; Spice 2005) using the default point source extraction widths. For the high resolution data, the point spread function nearly fills the high resolution slit length, so it is not possible to perform background subtraction using nod pairs. Instead, separate sky observations were used to construct a master sky that was subtracted from the individual BCDs to remove the background contribution. Extraction was performed in the same manner as for the low resolution modules. For both resolution regimes the extracted, background-corrected data were combined, using a weighted linear mean, into a single output data file. The point-to-point errors were estimated from the standard deviation of the flux at each wavelength bin except when there were fewer than three data points in which case the errors generated by the SSC pipeline were added in quadrature to determine the final error. For the high resolution modules, in the order overlap regions, the long wavelength edge of the orders were much less reliable than the short wavelength edges, and so only the short wavelength regions of overlap were retained, i.e. the data from the lower order. As suggested by the SSC, data outside the ranges 5.2–14.5 μm for the SL module, 9.9–19.6 μm for the SH module, and 14.0–38.0 μm and 18.7–37.0 μm for the LL and LH modules, respectively, were discarded as unreliable. The spectral lines were fit using a least squares Gaussian routine that fit the line center, line amplitude, continuum amplitude and the slope of the continuum. Individual segments of the IRS spectrum were shifted upwards or downwards by $\lesssim 10\%$ to ensure that segments

¹ssc.spitzer.caltech.edu/irs/dh/PDD.pdf

joined smoothly. The spectrum for 2006 April 16 is shown in Fig. 1; the spectrum for 2006 April 26 is not substantially different.

2.2. Ground-based observations

The SpeX/IRTF data were obtained on 2006 May 1 ($t = 77.61$ days) and June 3 ($t = 110.72$ days), UT using a $0.8'' \times 15''$ slit and a $10''$ N–S nod for background cancellation. No chopping was performed and extinction corrections were not necessary because of the proximity of the calibrator star. Data reduction was done using SpeXTools (Cushing et al. 2004) with HD164716 (B9V) as the calibrator star. The flux of HD164716 was obtained by using the Kurucz (1991; 1994) model of α Lyr scaled to the V magnitude of HD164716. SpeXTools makes an automatic, and in this case small, correction for extinction based on the measured $(B - V)$ colors. UKIRT observations were performed on 2006 April 16 and 24 ($t =$ days 62.72 and 70.66 respectively) using the UIST instrument; details of the observations and data reduction are given in Paper I. The spectra from both telescopes, in the $1\text{--}2.6\,\mu\text{m}$ and $2.8\text{--}4.0\,\mu\text{m}$ ranges, are shown in Figs. 2.

Optical ($BVr'i'z'$) photometry was obtained by the robotic 2m Liverpool Telescope (LT; Steele et al. 2004), sited on the island of La Palma, Canaries. Observations commenced as soon as RS Oph had declined to a level that would not saturate the detectors; standard photometric reduction techniques were used.

3. Discussion

The IR spectrum contains numerous emission lines. In the Spitzer wavelength range these lines are superimposed on a continuum that declines with increasing wavelength as $f_\lambda \propto \lambda^{-2}$, consistent with free-free emission. The emission lines include hydrogen recombination lines, together with fine structure lines, many of which are coronal; the hydrogen lines and free-free emission will be discussed elsewhere. We use flux ratios for lines from the same atomic species and within the same wavelength band to estimate the electron temperature in the region in which they originate; the line pairs are listed in Table 1. In Paper I the $[\text{Si}\,\text{vi}]/[\text{Si}\,\text{x}]$ flux ratio enabled us to estimate the temperature of the shocked, IR-emitting gas, to be $\simeq 9.3 \times 10^5$ K.

In this paper we have a wide range of ionic species and ionization stages at our disposal from which to estimate the electron temperature. Table 1 summarizes the collision strengths (Ω) at 10^5 K (Paper I) for the species and ionization stages observed in the IR spectra. This

temperature is the highest in these sources available in common to all species and stages of ionization, and the temperature-dependence of Ω is relatively weak. The ionization fractions are from Sutherland & Dopita (1993). The [Mg VII]5.50 μm feature is blended with the H 16-7 recombination line ($\lambda = 5.52 \mu\text{m}$) at the resolution of the Spitzer SL mode. To correct for this we assume Case B (Osterbrock & Ferland 2006), to estimate the expected flux ratio $f(\text{H16-7})/f(\text{H9-7}) \simeq 0.19$ at electron density $2 \times 10^5 \text{ cm}^{-3}$ (see below); we use the measured flux in the H 9-7 line ($\lambda = 11.31 \mu\text{m}$) to correct the [Mg VII] line for the blend with H 16-7. In view of the uncertainties (particularly in the applicability of Case B) we should give the temperature derived from the Mg lines lower weight than that derived from other species.

The derived temperatures are given in Table 1 (column 4). The uncertainties in $\log T(\text{K})$ arising from uncertainties in the line fluxes are ± 0.2 . We note that the temperatures in Table 1, derived from the Ne lines (mean $\simeq 1.5 \times 10^5 \text{ K}$), are lower than those derived from Si and Mg lines. The temperature derived from the Si lines in this paper is not significantly different from that given in Paper I during the early ($t = 55.7$ days) phase. Apparently there is a range of T values present in the shocked region. This result, derived from analysis of the IR emission lines, is also suggested by x-ray data obtained on 2006 April 16 (Osborne et al. 2006) and follows naturally from models of the shock in RS Oph (O'Brien et al. 1992).

We shall assume that the electron temperature in the region in which the various Ne and [O IV] lines originate is $1.5 \times 10^5 \text{ K}$, while that in the Si/Mg line emitting region is $9 \times 10^5 \text{ K}$. The resulting critical densities n_c , below which radiative de-excitation begins to dominate over collisional de-excitation at the assumed temperatures, are given in Table 2.

We use the fluxes in the [Ne V]14.3,24.3 μm lines to estimate the electron density in the ‘cooler’ line-emitting region. Denoting the ${}^2\text{P}_2$, ${}^2\text{P}_1$ and ${}^1\text{P}_0$ levels as levels ‘2’, ‘1’ and ‘0’ respectively, the fluxes f in the $14.32 \mu\text{m}$ and $24.3 \mu\text{m}$ lines are

$$f = n_u \frac{hc}{\lambda} A \frac{V}{4\pi D^2} , \quad (1)$$

where n_u (in cm^{-3} , $u = 2, 1$) is the population of the upper level, λ is the wavelength, A (s^{-1}) is the appropriate Einstein coefficient, V is the emitting volume and D ($= 1.6 \text{ kpc}$; Bode 1987) is the distance. Assuming that the [Ne V]14.2,24.3 μm lines arise in the same region, the flux ratio gives $n_2/n_1 \simeq 0.6$. Detailed balance between radiative de-excitation, and electron collisional excitation and de-excitation amongst the three levels, together with the above values for n_2/n_1 and the electron temperature, provide a value for the electron density n_e . We find $n_e \simeq 2.2 \times 10^5 \text{ cm}^{-3}$ in the [Ne V] emitting region.

On the basis of radio imaging of the ejecta, O'Brien et al. (2006) estimate that the density in the radio-emitting shell was $\sim 10^{-17} \text{ g cm}^{-3}$ at $t \simeq 14$ days. The wind/ejecta geometry is known to be complex (Bode et al. 2007); however assuming that the density

declines as t^{-2} (appropriate for a uniformly expanding shell of constant thickness), we expect the electron density would be $\sim 3 \times 10^5 \text{ cm}^{-3}$ at $t \simeq 63$ days, consistent with our estimate from the Ne lines. From Table 2 we see that this is generally below the critical density for all Ne lines with the exception of [Ne V]24.3 μm , the weakness of which compared with the other Ne lines may be consistent with a degree of collisional de-excitation.

We estimate the mass of emitting Ne, assuming that $n_0 + n_1 + n_2 = n([\text{Ne V}])$, and using the [Ne V] fluxes from Table 2 and equation (1). We find $n([\text{Ne V}]) \simeq 8.4 \times 10^{-9} \text{ M}_\odot$ for a distance of $D = 1.6$ kpc and, using the fractional abundance of [Ne V] at 1.5×10^5 K from Sutherland & Dopita (1993), we get $M(\text{Ne}) \simeq 2 \times 10^{-7} (D/\text{kpc})^2 \text{ M}_\odot$. In principle, we could also determine the mass of O; however it is clear from Table 2 that the deduced n_e in the Ne/O region exceeds the n_c for the $^2\text{P}_{3/2}$ state of [O IV]. Consequently we conclude only that $M(\text{O}) \gtrsim 1 \times 10^{-7} (D/\text{kpc})^2 \text{ M}_\odot$.

In principle it would be straightforward to use the fluxes in the IR Ne (and other species) lines, together with the fluxes in the H lines, to estimate the Ne:H ratio in the ejecta/wind mix. However given the complex geometry of the ejecta as evidenced by the radio (O'Brien et al. 2006) and HST (Bode et al. 2007) observations we do not consider that this is justified until we have a better understanding of the environment of RS Oph. However assuming that the emitting volumes of Ne and O coincide, we find $n(\text{O})/n(\text{Ne}) \gtrsim 0.6$, compared with a $\{n(\text{O})/n(\text{Ne})\}_\odot$ of 6.6 (Asplund et al. 2005).

In Fig. 3 we plot the time-dependence of the coronal line fluxes for which we have the longest time-base, namely S and Si; line fluxes for earlier data are taken from Paper I. It is curious that the S line fluxes decline monotonically over the first ~ 80 days of the eruption whereas there is a distinct minimum in the line fluxes around $t \simeq 70$ days for the Si lines (the errors in the measured fluxes are typically $\simeq 5\%$). We consider that this result is real, because (a) there is a consistent pattern in the behavior of the Si and S lines and (b) it coincides (within the time resolution) with a distinct ‘kink’ in the $BVr'i'z'$ light curves. There is no corresponding break in either the x-ray light curve (which coincides with the decline of the Super Soft phase; Ness et al. 2007) or in the variation of the hardness ratio (Osborne et al. 2007, see Fig. 3, which shows only the V and B light curves for clarity).

In *classical* novae, fluctuations in the visual light curve are often related to fluctuations in the mass-loss from the WD and the behavior of the pseudophotosphere; however, it is difficult to see how this can also lead to changes in the coronal line fluxes. Accordingly we consider it unlikely that this behavior is directly related to the mass-loss.

For the 1985 eruption of RS Oph, O'Brien et al. (1992) estimated that breakout of the shock from the edge of the RG wind occurred ~ 60 -70 days after the eruption, corresponding

to 70-80 days after the 2006 eruption, allowing for the greater inter-eruption interval. While this is close to the day 70 event in the 2006 eruption, it is unlikely that the behavior seen in Fig. 3 is related to any simple breakout phenomenon, which will be far more complex than the spherically symmetric model of O’Brien et al. (1992). Further, while the electron density we determine is for the Ne/O region, it is likely that this value is not atypical and the disparity between the n_c (Table 2) and n_e values suggest that the behavior depicted in Fig. 3 is not a collisional de-excitation effect. Fig. 3 suggests we may be seeing the combined effects of recombination, abundance gradients and element segregation, but a detailed discussion is beyond the scope of this paper.

4. Concluding remarks

We have presented the Spitzer IRS spectrum of RS Oph during its 2006 eruption, the first mid-IR observations of a RN in outburst. The IR spectrum, from $1\,\mu\text{m}$ to $30\,\mu\text{m}$, shows the rich fine structure (including) coronal and H recombination line spectrum of the shocked RG wind. There are at least two temperature regimes in the shocked wind, and the deduced electron density is consistent with extrapolation from radio observations earlier in the eruption.

This work is based in part on observations made with the Spitzer Space Telescope, which is operated by the Jet Propulsion Laboratory, California Institute of Technology under a contract with NASA. We acknowledge the award of Director’s Discretionary Time for this program. The United Kingdom Infrared Telescope is operated by the Joint Astronomy Centre on behalf of the U.K. Particle Physics and Astronomy Research Council (PPARC). The Liverpool Telescope is operated on the island of La Palma by Liverpool John Moores University in the Spanish Observatorio del Roque de los Muchachos of the Instituto de Astrofísica de Canarias with financial support from the UK Science and Technology Facilities Council. TRG is supported by the Gemini Observatory, which is operated by the Association of Universities for Research in Astronomy, Inc., on behalf of the international Gemini partnership of Argentina, Australia, Brazil, Canada, Chile, the United Kingdom, and the United States of America. CEW, AH and RDG are supported by NASA/JPL Spitzer contracts. The work of DKL, RJR and RWR is supported by The Aerospace Corporation’s Independent Research and Development Program. MFB was supported by a PPARC Senior Fellowship. J.-U. N. gratefully acknowledges support provided by NASA through Chandra Postdoctoral Fellowship grant PF5-60039 awarded by the Chandra X-ray Center, which is operated by the Smithsonian Astrophysical Observatory for NASA under contract NAS8-03060. JPO and KLP acknowledge support from PPARC. SGS acknowledges partial support from NSF and

NASA grants to Arizona State University.

Facilities: Spitzer (IRS), UKIRT, IRTF, Liverpool Telescope.

REFERENCES

- Asplund, M., Grevesse, N., Sauval, A. J., 2005, in *Cosmic Abundances as Records of Stellar Evolution and Nucleosynthesis*, eds F. N. Bash, T. G. Barnes, ASP Conference Series, Vol. 336, p. 25
- Berrington, K.A., Saraph, H.E., & Tully, J.A., 1998, A&AS, 129, 161.
- Bode, M. F., Kahn, F., 1985, MNRAS, 217, 205
- Bode, M. F., 1987, Ed, *RS Ophiuchi and the recurrent nova phenomenon*, VNU Science press, Utrecht
- Bode, M. F., et al., 2006, ApJ, 652, 629
- Bode, M. F., et al., 2007, ApJ, submitted
- Butler, K., & Zeippen, C.J., 1994, A&AS, 108, 1.
- Cushing, M. C., Vacca, W. D., Rayner, J. T., 2004, PASP, 116, 362
- Das, R., Banerjee, D. P. K., Ashok, N. M., 2006, ApJ, 653, L141
- Evans, A., et al., 2007, MNRAS, 374, L1 (Paper I)
- Fekel, F. C., Joyce, R. R., Hinkle, K. H., Skrutsie, M. F., 2000, AJ, 119, 1375
- Gehrz, R. D., et al., 2007, Rev. Sci. Instrum., 78, 011302
- Griffin & Badnell, 2000, J. Phys. B, 33, 4389.
- Griffin et al., 2001, J. Phys. B, 34, 4001.
- Houck J. R., et al., 2004, ApJS, 154, 18
- Hirosawa, K., 2006, IAUC8671.
- Kurucz, R.L., 1991, in Precision Photometry, eds A.G.D. Philip, A.R. Upgren, K.A. Janes (Schenectady: L. Davis), page 27

- Kurucz, R.L., 1994, Smithsonian Astrophys. Obs., CD-ROM No. 19.
- Lennon & Blair, 1994, A&AS, 103, 273
- Lynch, D. K., Rudy, R.J., Venturini, C.C., S. Mazuk, R.C. Puetter, 2001, AJ, 122, 213.
- Mitnik et al., 2001, J. Phys B, 34, 4455
- Ness et al., 2007, ApJ, in press.
- O'Brien, T.J., Bode, M.F., Kahn, F.D., 1992, MNRAS, 255, 683.
- O'Brien et al., 2006, Nature, 442, 279.
- Osborne et al., 2006, ATEL, 764.
- Osborne et al., 2007, to be submitted.
- Osterbrock, D. E., & Ferland, G. J., 2006, *Astrophysics of Gaseous Nebulae and Active Galactic Nuclei*, University Science Books, Sausalito, California.
- Rudy, R.J., Catherine C, Venturini, David K. Lynch, S. Mazuk, R.C. Puetter, 2002, ApJ, 573, 794.
- Shore, S. N., Kenyon, S. J., Starrfield, S., Sonneborn, G. 1996, ApJ, 456, 717
- Sokoloski et al., 2006, Nature, 442, 276
- Spice, 2005, Spice User's Guide, Version 1.1, <http://ssc.spitzer.caltech.edu/postbcd/spice.html>
- Steele, I. A., et al., 2004, SPIE, 5489, 679
- Sutherland, R. S., & Dopita, M. A., 1993, ApJS, 88, 253
- Starrfield, S., Sparks, W. M., Shaviv, G., 1988, ApJ, 325, L35
- Werner M. W., et al., 2004, ApJS, 154, 1
- Zhang, H.L., Graziani, M., & Pradhan, A.K., 1994, A&A, 283, 319.

Table 1: Estimated temperatures from coronal lines.

Line ratio	Flux ratio	Ω at 10^5 K ^a	$\log T$ (K)
[Si VI]1.96 μ m/[Si X]1.43 μ m	0.26	0.43, 0.13	5.96
[Mg VII]5.50 μ m/[Mg V]5.61 μ m	3.25	1.36, 1.06	5.85
[Ne III]15.55 μ m/[Ne V]14.32 μ m	1.18	0.79, 2.16	5.18
[Ne III]15.55 μ m/[Ne V]24.32 μ m	4.53	0.79, 0.75	5.15
[Ne VI]7.65 μ m/[Ne III]15.55 μ m	7.29	1.70, 0.79	5.34
[Ne II]12.81 μ m/[Ne V]14.32 μ m	0.99	0.40, 2.16	5.08

^aFrom Berrington, Saraph & Tully (1998) ([Si VI]), Butler & Zeippen (1994) ([Mg V], [Ne III]), Griffin et al. (2001) ([Ne II]), Griffin & Badnell (2000) ([Ne V]), Lennon & Blair (1994) ([Mg VII]), Mitnik et al. (2001) ([Ne VI]), Zhang, Graziani & Pradhan (1994) ([Si X]).

Table 2: Critical densities

Identification	Term	$\lambda(\mu\text{m})$	n_c (cm $^{-3}$) ^a
[Si X]	$^2\text{P}_{3/2}^o - ^2\text{P}_{1/2}^o$	1.4290	1.0×10^{10}
[Si VI]	$^2\text{P}_{1/2}^o - ^2\text{P}_{3/2}^o$	1.9625	1.7×10^9
[Si VII]	$^3\text{P}_0 - ^3\text{P}_2$	2.4822	7.0×10^8
[Mg VIII]	$^2\text{P}_{3/2}^o - ^2\text{P}_{1/2}^o$	3.0269	2.6×10^8
[Si IX]	$^3\text{P}_0 - ^3\text{P}_1$	3.7495	4.5×10^8
[Ne II]	$^2\text{P}_{1/2} - ^2\text{P}_{1/3}$	12.808	2.8×10^6
[Ne V]	$^3\text{P}_2 - ^3\text{P}_1$	14.311	1.4×10^5
[Ne III]	$^3\text{P}_1 - ^3\text{P}_2$	15.550	8.1×10^5
[Ne V]	$^3\text{P}_1 - ^3\text{P}_0$	24.300	2.4×10^4
[O IV]	$^2\text{P}_{3/2} - ^2\text{P}_{1/2}$	25.871	2.0×10^4

^aAt 1.5×10^5 K, for Ne/O lines, at 9×10^5 K for Si/Mg lines; see text.

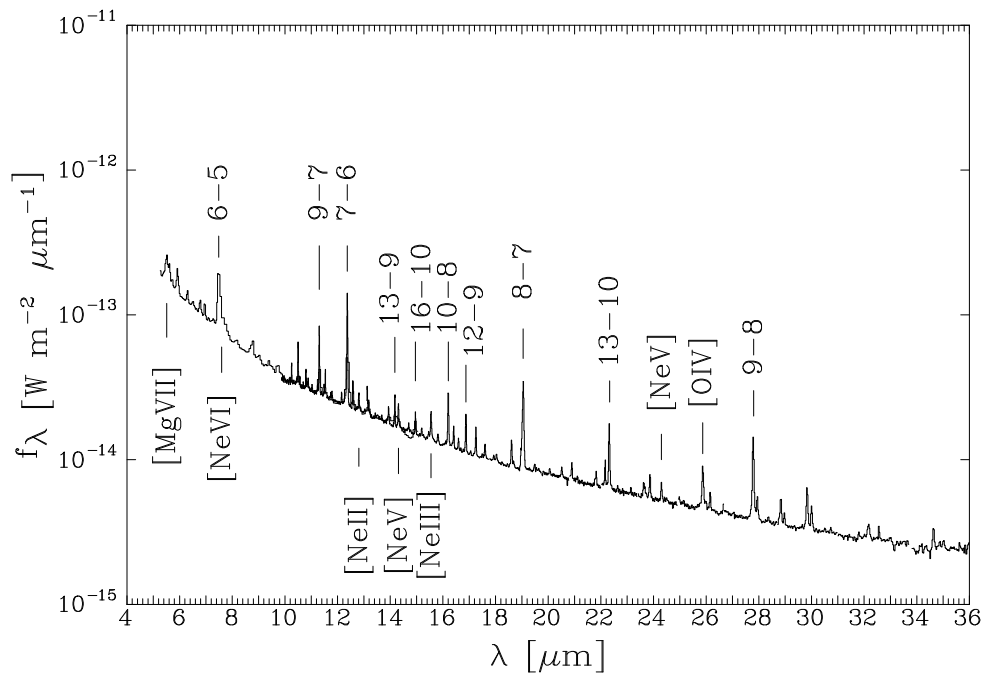


Fig. 1.— Spitzer spectrum of RS Oph for 2006 April 16 UT. Principal H recombination ($n - m$) and fine structure lines are identified; many of the lines without identification are also H recombination lines originating in high ($n \geq 15$) levels.

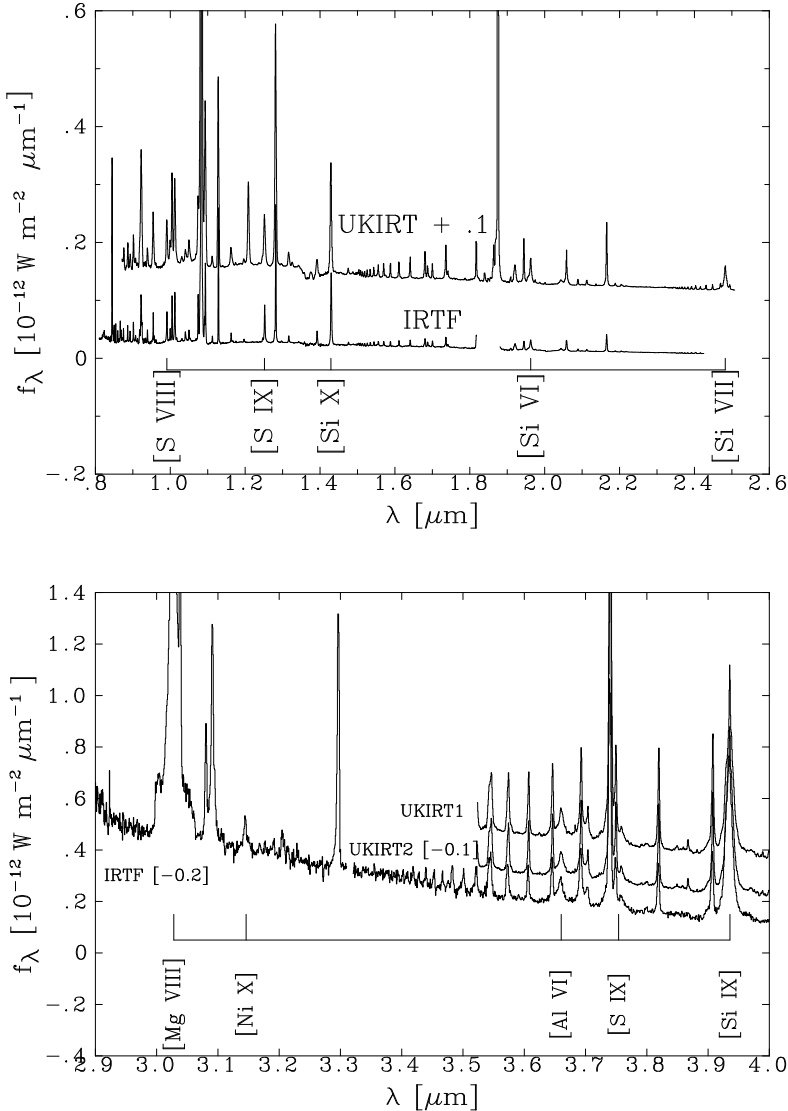


Fig. 2.— Top: Ground-based (UKIRT and IRTF) observations of RS Oph, obtained on 2006 April 24 (UKIRT) and May 1 (IRTF); UKIRT spectrum has been displaced upwards by $0.1 \times 10^{-12} \text{ W m}^{-2} \mu\text{m}^{-1}$. Coronal lines are identified. Bottom: Ground-based (UKIRT1, UKIRT2 and IRTF) observations of RS Oph, obtained on 2006 April 16 (UKIRT1), April 24 (UKIRT2) and May 1 (IRTF); spectra UKIRT2 and IRTF have been displaced downwards by $0.1 \times 10^{-12} \text{ W m}^{-2} \mu\text{m}^{-1}$ and $0.2 \times 10^{-12} \text{ W m}^{-2} \mu\text{m}^{-1}$ respectively. Coronal lines are identified. Many of the narrow lines without identification are H recombination lines. All dates UT.

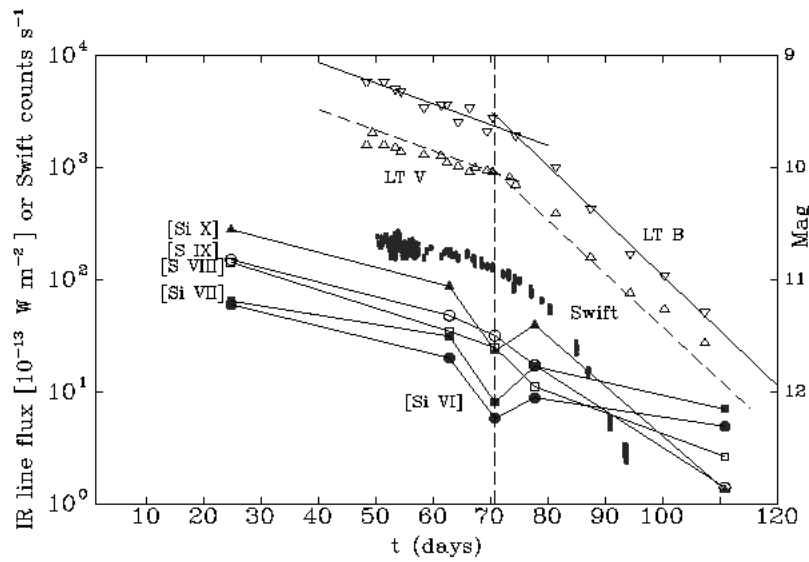


Fig. 3.— Decline in coronal line fluxes (\bullet = [Si VI], \circ = [Si VII], \square = [Si VIII], \blacktriangle = [Si IX], \blacksquare = [Si X]); ordinate (left axis) is line flux in $10^{-13} \text{ W m}^{-2}$. Swift fluxes in 0.3-10 keV channel (filled points); ordinate (left axis) is in counts s^{-1} . Liverpool Telescope (BV) light curves (open triangles; right axis); B data have been displaced upwards by 1.5 mag for clarity. Straight lines are least squares fits to light curves for the $40 < t$ (d) < 75 , $75 < t$ (d) < 120 ranges, illustrating break in the light curve around $t \simeq 70$ days. See text for discussion.